Light Metals 2014
Edited by: John Grandfield
TMS (The Minerals, Metals & Materials Society), 2014

Light Metals 2014

LIGHT-METAL MATRIX (NANO)-COMPOSITES

In-Situ Synthesis and Novel Additions

SESSION CHAIR
Dmitry Eskin
Brunel University
Uxbridge, United Kingdom

Light Metals 2014
Edited by: John Grandfield
TMS (The Minerals, Metals & Materials Society), 2014

Novel Ultrafine-Grained Aluminium Metal Matrix Composites Prepared from Fine Atomized Al Powders

M. Balog[1], F. Simancik[1], P. Krizik[1], M. Nosko[1], W. Rajner[2], M. Walcher[2], M. Qian[3]

[1]Institute of Materials and Machine Mechanics, The Slovak Academy of Sciences, Racianska 75, 83102 Bratislava, Slovakia
[2]New Materials Development GmbH, Römerstrasse 28, 83410 Laufen – Leobendorf, Germany
[3]School of Aerospace, Mechanical and Manufacturing Engineering, Design Research Institute, RMIT University, Melbourne, VIC 3001, Australia

Keywords: aluminium (Al), in-situ, metal matrix composites (MMCs), powder metallurgy (PM), ultrafine-grained (UFG)

Abstract

The paper reviews the developments to date of novel ultrafine-grained (UFG) Al metal matrix composites (MMCs) reinforced and stabilized with nanometric Al_2O_3 phase produced in situ by compaction of fine gas-atomized Al powders. This is followed by a discussion of the recent developments of the novel UFG Al-AlN MMCs produced by partial nitridation of fine gas-atomised Al powders. The paper summarizes previously published data with an addition of the new unpublished results.

1. Introduction

With the rising energy-saving concerns, it is in immediate need to build light-weight structural parts using high strength materials with expected service at elevated temperatures. Aluminium (Al) alloys are widely used in the transportation industry due to their high specific strength. However, high strength Al alloys show a pronounced strength loss at relatively low temperatures (~150 °C) due to overaging effects. This loss limits the application of high strength Al alloys that requires performance at elevated temperatures (e.g., engine parts such as pistons, liners, etc.). The thermal stability of Al alloys can be improved by introducing transition metals with low diffusivity in Al, such as Ni, Cr, Mn, and Fe. However, the limited solubility limits of these metals in Al restrict their effectiveness. Hence, the service temperature limit of reference for thermally stable Al-based alloys, such as A2024, A2618, and A2650, is still below 200 °C [1].

"Sintered Aluminium Powder" (*SAP*) materials prepared via powder metallurgy route gained considerable attention in the middle of the last century [2]. *SAP* materials offer superior mechanical properties, enhanced creep performance and increased thermal stability at elevated temperatures after prolonged high temperature exposures. They include a broad range of dispersion-strengthened Al-Al_2O_3 composites produced primarily from mechanically milled or further oxidised Al powders [3]. However, the mechanical properties of such *SAP* materials are not always reproducible, and the cost of production is high. These issues prohibited the widespread use of *SAP* materials in the last century.

High quality fine Al powder produced by gas-atomization is now available in commercial quantities at an affordable price. Consolidation of such fine Al powder via plastic forming allows the fabrication of UFG Al composites reinforced with nanometric Al_2O_3 dispersoids, which are a result of the fragmented thin (~2 nm) native oxide films on the Al powder [4, 5, 6]. Such Al-Al_2O_3 composites, named "High Temperature Aluminium" (*HITEMAL*), possess superior tensile and creep performance and thermal stability at elevated temperatures due to the unique strengthening and stabilizing effects of the nanometric Al_2O_3 particles along the boundaries of the submicrometric Al grains [7]. The quantity and distribution of such nanometric Al_2O_3 dispersoids largely dictate the mechanical properties of the composites [8]. Due to the unique strengthening and stabilizing effects of the Al_2O_3 dispersoids *HITEMAL* materials show superior or similar properties to *SAP* fabricated from milled or additionally oxidized Al powder, in addition to simplified processing steps and reduced cost of fabrication.

This paper reviews the developments of *HITEMAL* materials made over the last decade and MMCs which are essentially based on the *HITEMAL* concept. Some data included in this paper have been previously published elsewhere [4, 7-10].

2. Experimental

Fine air-atomized commercially pure (CP) Al powders (99.8% purity; d_{50}=1-10 μm)), supplied by New Materials Development GmbH [11], were used. The particle size distribution (PSD) was analysed by a laser diffraction system by wet dispersion (Fritsch machine). The equivalent BET diameter (d_{BET}, μm) was calculated according to the relation $d_{BET} = 6 / (BET \cdot \rho_{Al})$, where ρ_{Al} is the density of Al (2.7 $g.cm^{-3}$) and BET ($m^2.g^{-1}$) is the powder surface area determined by physical adsorption with multipoint Brunauer, Emmett, Teller analysis. The oxygen content of the as-atomised powders was measured by hot gas extraction using a Ströhlein machine. The Al_2O_3 volume was calculated from the oxygen content detected on as-atomized powders and d_{BET}. All detected oxygen was assumed to be present as Al_2O_3.

Loose powder was cold isostaticaly pressed (CIP) at 2OO MPa. CIP green compacts were subjected to vacuum degassing at 420 °C for 12 h under a vacuum of 5.10^{-2} Pa prior to compaction. Degassed green compacts were compacted either by direct extrusion (DE), quasistatic forging (F) or hot isostatic pressing (HIP). DE was performed at an extrusion temperature of 450 °C and an average ram speed of ~1 $mm.s^{-1}$ with an extrusion ratio of R = 11:1. Quasistatic forging compaction was performed using a Lasco SPR 1000 screw press at 57 kJ press energy and a maximal speed of 550 $mm.s^{-1}$. The forging die was preheated to 110 °C. The die walls were lubricated by graphite water solution. HIP was performed at 500 °C under 100 MPa pressure for 2 hours dwell. Vacuum sintering of CIP green compacts was carried out at 590 °C for 2 hours of dwell time and 10^{-3} Pa vacuum. *HITEMAL_2.3* refers to the fine Al powder compacts with 2.3 vol.% of Al_2O_3.

Nitridation of CIP green compacts, fabricated from fine Al99.8% powder of d_{50}=1.31 μm, was conducted in a tube furnace, which was evacuated to 5 Pa before the samples were placed in. Up to 0.5wt.% Sn powder (<45 μm) was mixed into the fine Al powder to control the growth of the AlN layer during nitridation. The green compacts containing 0.3%Sn and 0.4%Sn were first heated to 350 °C at 15 $°C.min^{-1}$ in vacuum for degassing. Then nitrogen (99.99% purity) was introduced at a flow rate of 2 $l.min^{-1}$ and the samples were heated to 590 °C at 15

°C.min^{-1} for 120 min of nitridation. The resulting AlN content was calculated according to the weight gain after nitridation. The partially nitrided samples were consolidated by DE, where the samples were placed in a die preheated to 480 °C and held at temperature for 30 min prior to extrusion into Al-AlN MMCs profiles. For further experimental details please see References [4, 7, 8, 10].

3. Results and discussion

3.1 As-atomized fine Al powders

Market survey revealed 35 different types of gas (air, nitrogen) atomized Al powder products of technical purity (99.5 - 99.8%) with the median particle size d_{50} spanning between 1–10 µm, produced by 12 worldwide manufacturers. The morphology of selected as-atomized Al powders is shown in **Figure 1**. The powder particles with d_{50} < ~3 µm were largely spherical and the coarser powder particles with d_{50} > ~3 µm were mainly irregular but still rounded. A few small satellites were found attached onto the surfaces of some powder particles. Depending on the powder source, PSD analyses revealed normal as well as multimodal (bimodal, trimodal) particle size distributions of tested powders. Size distribution depends on the powder filtration and collection systems used. Characterization of as-atomized powders revealed an almost linear correlation between the oxygen content and the powder specific surface area BET (e.g. d_{BET}), see **Figure 2**. The thickness of the native Al_2O_3 layer on as-atomised powders was calculated to be 2.3±0.7 nm from the oxygen content and BET data. Even for the finest commercially available gas-atomized Al powder, the native Al_2O_3 layers are limited to < 2.3vol.%. TGA analyses indicated that the native Al_2O_3 is mostly amorphous and undergoes gradual transition from amorphous to crystalline α-Al_2O_3 with increasing annealing temperature. These observations are consistent with other studies. Gas atmosphere had no apparent effect on the properties of the as-atomized powders [12, 13].

3.2 The effect of compaction technique

The powder compaction technique and processing parameters used strongly affect the microstructure of *HITEMAL*. In general, the microstructure of *HITEMAL* consists of Al grains stabilized with homogenously distributed nanometric Al_2O_3 particles, which are normally found at high angle grain boundaries (HAGBs) which may contain subgrains, i.e. low angle grain boundaries (LAGBs). The size and shape of the Al grains along with the morphology and distribution of the Al_2O_3 phase can be varied to a large extent by different consolidation processes. If sufficient shear deformation is introduced during hot working (such as extrusion or equal channel angular pressing - ECAP), the Al powder particles elongate and native Al_2O_3 layer are disrupted into separate nanometric plate-like dispersoids. The thickness of the plate-like dispersoids reflects the thickness of the native Al_2O_3 layer (~2 nm), **Figure 3a**. The transversal Al grain size is significantly reduced after extrusion compared to the median particle size. If the powders are extruded at sufficiently low temperatures (i.e., high deformation energy is induced during compaction), some Al_2O_3 dispersoids can be found in severely deformed Al grains. Conversely, quasistatic forging with limited shear yields a two-phase microstructure: polyhedral Al grains decorated with continuous Al_2O_3 skeletons (**Figure 3b**). Compaction by hot working techniques yields sound and dense (>99% THD) *HITEMAL*. Microstructures obtained after subsequent vacuum sintering or HIP recall those obtained after forging where the native Al_2O_3 layers fragmented and spheroidized into a large number of Al_2O_3 dispersoids along Al grain boundaries (**Figure 3c**) which prevent Al grains from growth during sintering or HIP. Selected area diffraction revealed the presence of α-Al_2O_3 (corundum) in *HITEMAL* produced by different compaction techniques.

The compaction technique used exerts a strong effect on the properties of *HITEMAL*. An example is demonstrated in **Figure 4**, where the mechanical properties of *HITEMAL_2.3* change markedly depending on the compaction technique used (forging, extrusion, HIP). Furthermore, the morphology of Al_2O_3 dispersoids affects other properties of *HITEMAL* including the creep performance, thermal stability and conductivity (thermal, electrical).

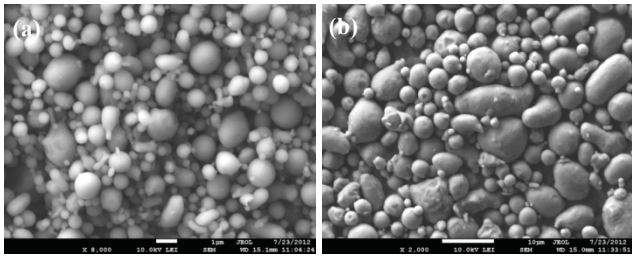

Figure 1. SEM images of loose gas as-atomised powders with d_{50} = 1.3 µm (a) and 8.9 µm (b).

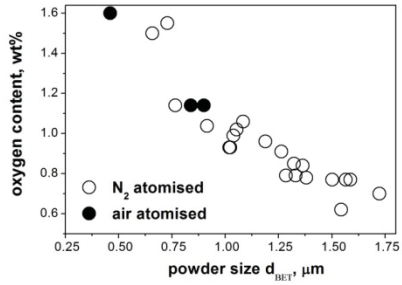

Figure 2. Oxygen content of the Al powder as a function of the specific surface area of the powder (i.e., powder diameter d_{BET}). (Redrawn from *Mater. Sci. Eng. A* Vol. 529, Balog et al., 131–137 (2011), with permission from Elsevier).

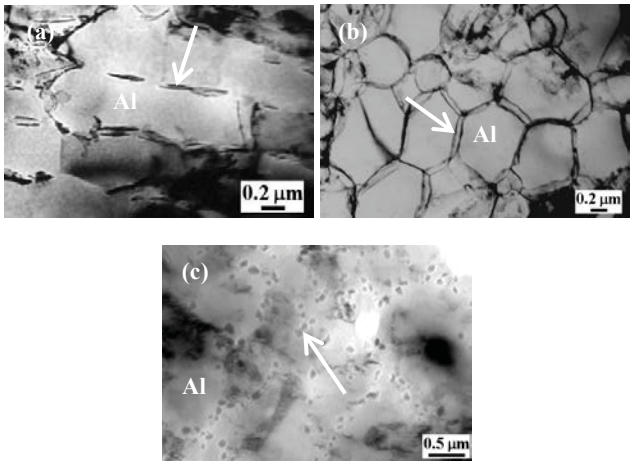

Figure 3. BF TEM images of *HITEMAL_2.3* produced via direct extrusion (a), forging (b), HIP (c). The arrows indicate Al_2O_3. (Reprinted from *J. Alloys Comp.* Vol. 509S, Balog et al., S235-S238 (2011), with permission from Elsevier).

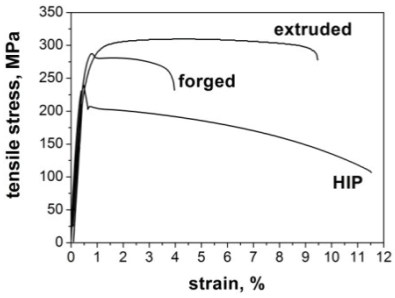

Figure 4. Room temperature stress-strain curves of as-processed (forged, extruded and HIPed) *HITEMAL_2.3* materials.

3.3 The effect of used Al powder on *HITEMAL* microstructure

The powder properties, namely the d_{50} and the d_{BET}, strongly affect the microstructure of *HITEMAL*. **Figure 5** shows the grain size of HAGBs (>11°) detected by SEM EBSD analyse (d_{EBSD}) and the content of LAGBs (3-11°) of five as-forged *HITEMAL* materials detected by EBSD. The portion of LAGBs is very low (1%) for *HITEMAL_2.3* produced from the finest powders and significantly increases (28%) for *HITEMAL_1.02* produced from the coarsest powder (**Figure 6**). The grain size (d_{EBSD}) increased from 0.53 (±0.3) µm for *HITEMAL_2.3* to 1.51 (±1.1) µm for *HITEMAL_1.02*. As seen in **Figure 5**, d_{EBSD} increased with increasing size of the powder used and follows the BET (respectively d_{BET}) of the powder used. Similarly, the portion of LAGBs detected by EBSD increased with increasing d_{BET}. Similar tendencies were confirmed for highly deformed as-extruded *HITEMAL*.

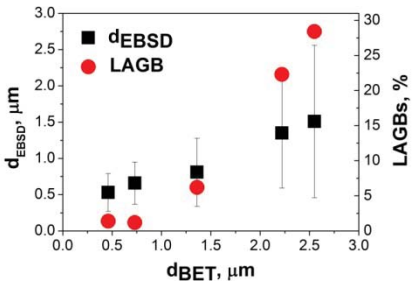

Figure 5. The grain size d_{EBSD} and the content of LAGBs (3-11°) of as-forged *HITEMAL* materials as a function of the specific surface area of the powder (i.e. d_{BET}).

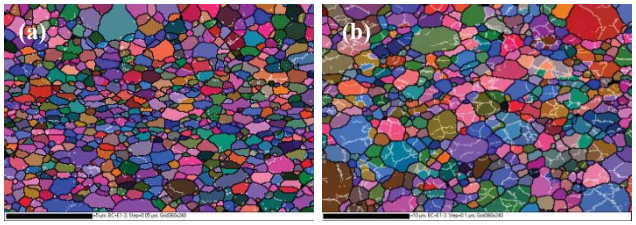

Figure 6. EBSD maps of as-forged *HITEMAL_2.3* (a) and *HITEMAL_1.02* (b) materials. The white and black lines in the maps represent LAGBs (3-11°) and HAGBs (>11°) of Al grains, respectively.

3.4 Properties of *HITEMAL* materials

3.4.1 Exceptional thermal stability

HITEMAL materials show exceptional thermal stability at elevated temperatures even after prolonged high temperature exposures. No major microstructural changes are detected after annealing of forged and extruded *HITEMAL* to 400 - 450 °C. Forged and extruded *HITEMAL* materials exhibit only one distinctive microstructural change upon annealing; the Al_2O_3, either in the form of continuous skeleton or plate-like dispersoids, transforms into discrete nanometric Al_2O_3 spherical particles (<100 nm) after 24 h annealing at 500 °C. **Figure 7** shows the microstructures of forged *HITEMAL* materials after annealing at 600 °C for 24 h. As confirmed by EBSD analyses, no obvious Al grain growth takes place after 24 h annealing at 600 °C. Spherical Al_2O_3 particles decorate HAGBs of Al grains whilst the Al grain size remains unchanged. The content of LAGBs does not changes either upon heating. HIP-processed or sintered *HITEMAL* materials which contain spherical Al_2O_3 dispersoids show no microstructural changes for long-term annealing up to 600 °C.

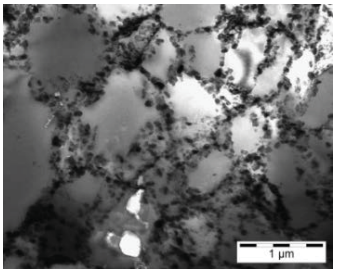

Figure 7. Bright field TEM images of forged *HITEMAL_2*.3 after annealing at 600 °C for 24 h.

3.4.2 High strength at elevated temperatures

HITEMAL materials show good strength levels at elevated temperatures. **Figure 8** shows the ultimate tensile strength (UTS) of extruded *HITEMAL_2.3* tested at temperatures up to 550 °C. The UTS decreases with increasing temperature. However, the extruded *HITEMAL_2.3* preserved UTS of 71 MPa at 500 °C, which is roughly the room temperature UTS of unreinforced A1050 alloy. The systematic study of the extruded *HITEMAL* materials revealed that the tensile strength is closely related to the specific surface area (d_{BET}) of the fine powder used. **Figure 9** summarizes the tensile properties of the as-extruded *HITEMAL*, tested at room temperature and 300 °C as a function of d_{BET}. The atomization gas showed no observable effect on the mechanical properties of the compacts. The strength of the compacts increased with decreasing d_{BET}, particularly when the d_{BET} values are below 1 µm. The relationship can be described as follows

$$UTS = a_1 \cdot d_{BET}^{-0.27}, \quad (1)$$

$$YS = a_2 \cdot d_{BET}^{-0.26}, \quad (2)$$

where the constants a_1 and a_2 are calculated to be 5.3 and 6, respectively, at room temperature, and 3.9 and 3.6, respectively, at 300 °C. **Figure 10** depicts the effect of the Al_2O_3 dispersoid volume fraction on the yield strength of as-extruded *HITEMAL* at room temperature and 300 °C. *HITEMAL* materials show similar or higher yield strength compared to high Al_2O_3 content SAP materials but they are achieved at a much smaller volume of Al_2O_3.

The strength of the fine Al powder compacts containing nanometric Al_2O_3 particles stems from the combination of several strengthening mechanisms. Its dependence on grain size is similar to the ultra-fine grained (UFG) materials fabricated by severe plastic deformation (SPD) and CP Al ingots [14, 15]. At the grain size of ~10 μm there is a sudden deviation from the conventional Hall-Petch relation

$$YS = \sigma_0 + k \cdot d_{EBSD}^{-0.5}, \quad (3)$$

where σ_0 is the flow stress for an infinite grain size, k is the constant determining the efficiency of grain boundaries as slip barriers. Here k suddenly increases from 44-68 MPa.μm$^{0.5}$ for coarse grained Al to 175 MPa.μm$^{0.5}$. Unlike UFG materials prepared by SPD of CP Al ingots, *HITEMAL* preserves this behaviour after passing the other critical grain size ~2 μm and YS still increases at k = 175 MPa.μm$^{0.5}$ rate. The results are in good correlation with data obtained on materials prepared by spark plasma sintering of fine Al powders [5].

The fracture strain of *HITEMAL* drops as the particle size decreases (**Figure 9**). The tensile elongation of UFG Al alloys reinforced with nanometric dispersoids decreases with increasing temperature, and with decreasing strain rate too [17]. This is in distinct contrast to conventional ingot metallurgy Al alloys. The same phenomena were also observed for *HITEMAL* (**Figure 8**). At testing temperatures >500 °C, virtually zero strain is measured at fracture. The mechanism remains unclear; reduced fracture resistance at elevated temperatures was speculatively attributed to strain localization and plastic instability between growing microvoids [16].

HITEMAL materials retain their mechanical properties (UTS, YS, ε and E) even after prolonged annealing at 400 and 450 °C for 24 h. However, long term annealing beyond the temperature of Al_2O_3 morphological transformation (i.e. Al_2O_3 spheroidization) yields some changes in mechanical properties. Thus, the tensile strength of forged and extruded *HITEMAL* annealed at 500 °C for 24 h decreases slightly compared to the as-fabricated and a gradual decrease in strength is confirmed with increased annealing temperature (**Figure 12**).

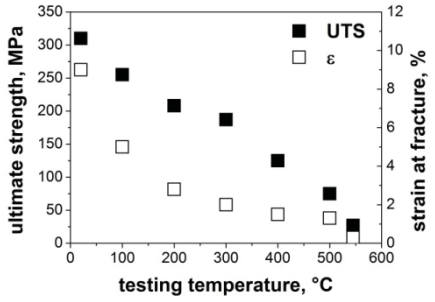

Figure 8. Ultimate tensile strength (UTS) and strain at fracture (ε) of extruded *HITEMAL_2.3* tested at different temperatures.

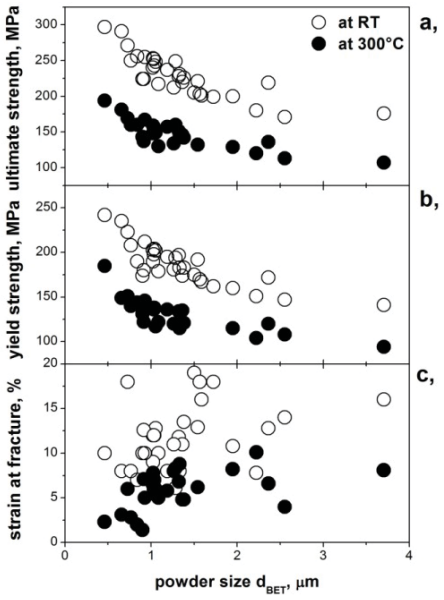

Figure 9. The effect of the specific surface area of the air and nitrogen atomised powders (i.e., powder diameter d_{BET}) on (a) ultimate tensile strength, (b) yield strength and (c) strain at fracture of extruded *HITEMAL* materials (tested at room temperature and at 300 °C). (Redrawn from *Mater. Sci. Eng. A* Vol. 529, Balog et al., 131– 137 (2011), with permission from Elsevier).

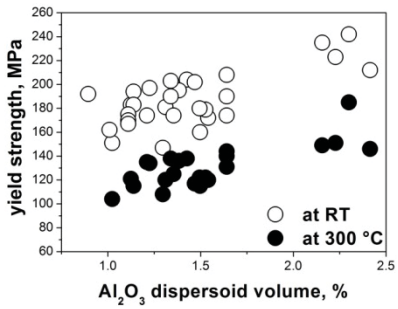

Figure 10. Yield strength of as-extruded *HITEMAL* (tested at room temperature and at 300 °C) as a function of Al_2O_3 dispersoid volume. (Redrawn from *Mater. Sci. Eng. A* Vol. 529, Balog et al., 131– 137 (2011), with permission from Elsevier).

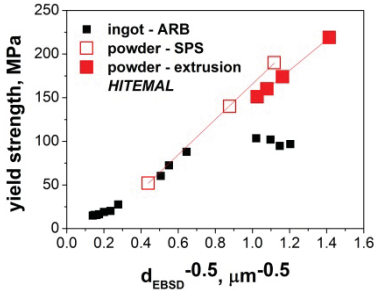

Figure 11. Relationship between yield stress and grain size (d_{EBSD}) of extruded *HITEMAL*. Data on Al ingot (99.99% purity) severely deformed by accumulative roll-bonding (ARB) [14] and fine Al

powders consolidated by spark plasma sintered (SPS) [5] are included for comparison.

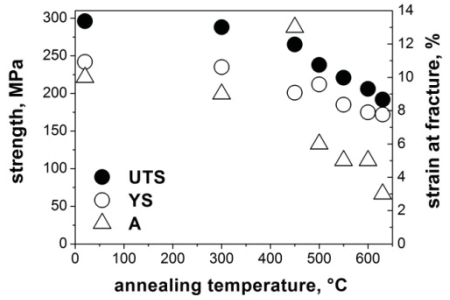

Figure 12. Mechanical properties of extruded *HITEMAL_2.3* as a function of annealing temperature; annealing time 24 hours (UTS – ultimate tensile strength, YS – yield strength, A – strain at fracture). (Redrawn from *Mater. Sci. Eng. A* Vol. 529, Balog et al., 131– 137 (2011), with permission from Elsevier).

3.4.3 Enhanced creep performance

Al_2O_3 dispersoids can act as effective barriers to grain boundary sliding which is the key creep resistance mechanism of fine grained Al based materials. Thus, UFG *HITEMAL* materials with stabilized grain boundaries show superior creep performance up to ~400 °C. The morphology of the Al_2O_3 phase rules the creep performance of *HITEMAL* significantly. In terms of the creep performance, as-forged *HITEMAL* stabilized with continuous Al_2O_3 skeleton has considerable higher creep stability compared to extruded and sintered counterparts with discrete Al_2O_3 dispersoids. The creep performance of *HITEMAL* is superior to the conventional heat resistant high strength Al alloys [18], see in **Figure 13**.

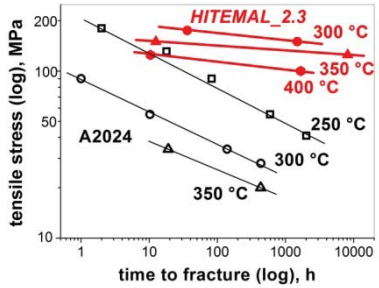

Figure 13. Stress rupture plots of forged *HITEMAL_2.3*. For a comparison data of conventional ingot based A2024 T851 alloy is shown [17]. (Redrawn from *Mater. Sci. Eng. A* Vol. 549, Cavojsky et al., 233-241 (2012), with permission from Elsevier).

3.5 *SAP* concept Al-AlN MMCs

The native Al_2O_3 films of *HITEMAL* are limited to < 2.3vol.%. Intentional oxidation or mechanical milling is often used to increase the volume fraction of the Al_2O_3 phase (*SAP* concept). However, *SAP* fabricated from milled or oxidized Al powder show inferior and inconsistent properties compared to *HITEMAL*, aside from the increased cost. To overcome this limitation, the native Al_2O_3 surface skins are replaced with in situ formed AlN surface skins [10]. Atmospheric nitridation in flowing nitrogen followed by hot working compaction (extrudion, forging) of partially nitrided fine Al powder green compacts is used to fabricate UFG Al-AlN nanocomposites. AlN has high elastic modulus, high strength, low density, low thermal expansion and good wear resistance. Hence it is a preferred reinforcement for Al. In situ formed AlN on Al powder ensures favourable Al-AlN interfacial bonding, which is essential for the fabrication of high performance Al-AlN nanocomposites [18].

Fine Al powders nitride readily at 590 °C in flowing nitrogen at atmospheric pressure. In order to bring the process into control and to enable homogenous nitridation throughout the green compacts a small addition of Sn powder (0.3-0.4wt.%) was introduced in Al powder green compacts. Fine Al powder can serve as a potent self-getter of the residual oxygen in the nitrogen and enables easy nitridation of the powder without the assistance of magnesium. Bright field TEM reveals that each Al particle shows a core-shell structure, where the core is the remnant of the original Al particle and the shell is a nitrided layer (**Figure 14**). The shell is ~150 nm thick. The nitrided layer on each fine Al powder particle has a composite structure of nanometric AlN crystals embedded in the Al matrix with some Al_2O_3 nanocrystals. Compaction realized by extrusion and forging led to full densification of partially nitrided Al-AlN green compacts. Extrusion resulted in slight elongation of the nitrided Al powder along the extrusion direction and fragmentation of some nitrided layers (**Figure 15**). The large volume fraction of the in situ formed AlN dispersoids and their excellent metallurgical bonding with the Al matrix resulted in largely improved tensile strength and Young`s modulus at 300 ºC compared to AlN free *HITEMAL* and *SAP* materials and coarse grained Al-AlN composites with similar contents of AlN. For instance the Al+13vol.% AlN nanoMMC fabricated by the this approach shows high tensile properties at 300 °C (UTS = 227 MPa, YS = 195 MPa and E = 66 GPa) and excellent thermal stability up to 500 °C (**Figure 15**).

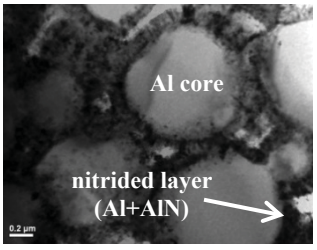

Figure 14. Bright field TEM micrographs of fine Al powder green compacts containing 0.3wt.% Sn precompacted by CIP and nitrided in flowing nitrogen. (Reprinted from *Mater. Sci. Eng. A* Vol. 588, Balog et al., 181-187 (2013), with permission from Elsevier).

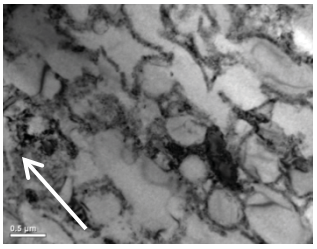

Figure 15. Bright field TEM micrographs of extruded Al-13vol.% AlN nanocomposites shown in longitudinal directions in relation to the extrusion axis (see the arrow). (Reprinted from *Mater. Sci.*

Eng. A Vol. 588, Balog et al., 181-187 (2013), with permission from Elsevier).

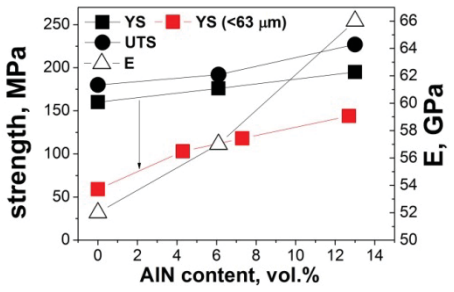

Figure 16. Ultimate tensile strength (UTS), yield strength (YS) and Young`s modulus (E) of extruded Al-AlN nanocomposites measured at 300 °C. YS data of Al-AlN (<63 μm) composites is included for comparison. (Redrawn from *Mater. Sci. Eng. A* Vol. 588, Balog et al., 181-187 (2013), with permission from Elsevier).

4. Summary

A review has been made of the developments to date of *HITEMAL* materials. The following conclusions were made.

- The Al_2O_3 content present on the surfaces of the as-atomised Al powders with the mean size in the range of d_{50} = 1-10 μm shows a linear correlation with the specific surface area of the powders. The thickness of the Al_2O_3 surface layers was calculated to be 2.3±0.7 nm.
- The microstructure of *HITEMAL* consists of (sub)micrometric Al grains (HAGBs) decorated with nanometric Al_2O_3 dispersoids. Al grains may contain substructures of LAGBs. The grain size and content of LAGBs of *HITEMAL* increase with increasing specific surface area of the powder.
- The powder compaction technique and parameters have a strong effect on the microstructure and properties of *HITEMAL*. The atomising atmosphere (nitrogen or air) has no significant effect on the properties of as-atomised powders and on the mechanical properties of *HITEMAL* materials.
- *HITEMAL* shows superior thermal stability, mechanical strength and creep performance up to ~425 °C.
- The mechanical strength of *HITEMAL* is strongly related to the specific surface area of the powder used for compaction. Strengthening by grain boundaries acts as a major strengthening mechanism.
- The elongation of *HITEMAL* materials decreases with increasing specific powder surface area and testing temperature and with decreasing strain rate.
- *SAP* concept Al-AlN nanocomposites can be fabricated via partial nitridation of fine gas-atomised Al powder green compacts in flowing nitrogen at atmospheric pressure, followed by hot direct extrusion. Al-AlN nanocomposites fabricated this way show excellent thermal stability up to 500 °C and largely improved tensile strengths and Young`s modulus at 300 ºC compared to *HITEMAL* and *SAP* materials.

References

1. J.S. Robinson, R.L. Cudd and J.T. Evans, Creep Resistant Aluminium Alloys and their Applications, *Mater. Sci. Tech.* 19 (2003) 143-155.
2. R. Irman, Sintered aluminium with high strength at elevated temperatures, *Metallurgia* 46 (1952) 125-133.
3. N. Hansen, Dispersion-strenghtened aluminium products, Risö Report No. 223, ISBN 8755000592 (1971)
4. M. Balog, C. Poletti, F. Simancik., M. Walcher and W. Rajner, The effect of native Al_2O_3 skin disruption on properties of fine Al powder compacts, *J. Alloys Comp.* 509S (2011) S235–S238.
5. G.M. Le, A. Godfrey and N. Hansen, Structure and strength of aluminum with sub-micrometer/micrometer grain size prepared by spark plasma sintering, *Materials & Design* 49 (2013) 360-367.
6. K. Xia and X. Wu, Back pressure equal channel angular consolidation of pure Al particles, *Scripta Mater.* 53 (2005) 1225–1229.
7. M. Balog, F. Simancik, O. Bajana and G. Requena, ECAP vs. direct extrusion—Techniques for consolidation of ultra-fine Al particles, *Mater. Sci. Eng. A* 504 (2009) 1-7.
8. M. Balog, F. Simancik, M. Walcher, W. Rajner and C. Poletti, Extruded Al–Al_2O_3 composites formed in situ during consolidation of ultrafine Al powders: Effect of the powder surface area, *Mater. Sci. Eng. A* 529 (2011) 131– 137.
9. C. Poletti, M. Balog, F. Simancik and H. P. Degischer, High-temperature strength of compacted sub-micrometer aluminium powder, *Acta Mater.* 58 (2010) 3781-3789.
10. M. Balog, P. Krizik, M. Yan, F. Simancik, G.B. Schaffer and M. Qian, SAP-like ultrafine-grained Al composites dispersion strengthened with nanometric AlN, *Mater. Sci. Eng. A* 588 (2013) 181-187.
11. http://www.nmd.at [accessed 17.9.2013]
12. B. Rufino, F. Boulc'h, M.-V. Coulet, G. Lacroix and R. Denoyel, Influence of particles size on thermal properties of aluminium powder, *Acta Mater.* 55 (2007) 2815–2827.
13. M. A. Trunov, S. M. Umbrajkar, M. Schoenitz, J. T. Mang and E. L. Dreizin, Oxidation and melting of aluminum nanopowders, *J. Phys. Chem. B* 110 (2006) 13094-13099.
14. N. Kamikawa, X. Huang, N. Tsuji and N. Hansen, Strengthening mechanisms in nanostructured high-purity aluminium deformed to high strain and annealed, *Acta Mater.* 57 (2009) 4198-4208.
15. C.Y. Yu, P.W. Kao and C.P. Chang, Transition of tensile deformation behaviors in ultrafine-grained aluminium, *Acta Mater.* 53, (2005) 4019-4028.
16. S. S. Kim, M. J. Haynes and R. P. Gangloff, Localized deformation and elevated-temperature fracture of submicron-grain aluminum with dispersoids, *Mater. Sci. Eng. A* 203 (1995) 256-271.
17. J.G. Kaufman, Parametric analyses of high-temperature data for aluminium alloys, first edition, ASM International, Ohio, (2008)
18. P. Yu, M. Balog, M. Yan, G.B. Schaffer and M. Qian, In-situ fabrication and mechanical properties of Al-AlN composite by hot extrusion of partially nitrided AA6061 powder, *J. Mater. Res.* 26 (2011) 1719-1725.

Acknowledgments

The visit of Martin Balog to The University of Queensland was funded by a Go8 European Fellowship. The financial support from VEGA 2/0116/11, SAS-NSC JRP 2011/06, ITMS 26240220073 and SRDA APVV-0556-12 projects is gratefully acknowledged.